The Influence of Intraparticle Diffusion in Fixed Bed Catalytic Reactors

SHEAN-LIN LIU

Mobil Research and Development Corporation, Princeton, New Jersey

By using curve fitting techniques, mathematical formulas are obtained for the catalyst effectiveness factors for nonisothermal first-order and second-order irreversible chemical reactions. The effects of intraparticle mass and heat diffusion upon the concentration and temperature profiles in adiabatic and nonadiabatic catalytic reactors are examined. A relation between the maximum interstitial adiabatic temperature and the maximum intraparticle temperature in the reactor is obtained. For some sets of parameters in a nonadiabatic reactor, the concentration and temperature and, consequently, the reactor effluent are sensitive to small changes in the properties of catalyst particles.

When a chemical reaction occurs within a relatively large porous catalyst particle, mass concentration and temperature gradients can exist within the particle. Because of these gradients, the actual reaction rate differs from the intrinsic reaction rate that would occur if the entire catalytic surface were exposed to the concentration and temperature conditions holding at the surface of the particle. The catalyst effectiveness factor η is defined as the ratio of the actual reaction rate to the intrinsic reaction rate. Damköhler (*9*) and Thiele (*18*) were the first to consider the effectiveness factor problem. Effectiveness factors under nonisothermal conditions have been discussed by Weisz and Hicks (*20*), Carberry (*6, 7*), and others (*8, 14, 17*).

The problem of the fixed bed reactor packed with large particles has been considered only for simplified models (*3, 4, 10* to *13*). Wendel and Carberry (*21*) considered the effect of intraparticle mass diffusion in a fixed bed catalytic reactor. The purpose of the work reported here is to study the effects of intraparticle mass and heat diffusion upon the concentration and temperature profiles in adiabatic and nonadiabatic catalytic reactors.

By using curve fitting techniques, empirical mathematical formulas for the effectiveness factors are obtained for nonisothermal first-order and second-order irreversible chemical reactions. These formulas for η are used in conjunction with mass and heat balances in the fluid phase to obtain solutions for the problems of catalytic reactors. One can save considerable amounts of computing time by using the formula for η, because it is not necessary to solve the two differential equations, a two-point boundary value problem, describing the intraparticle concentration and temperature at each point in the bed.

By analyzing the steady state equations for an adiabatic reactor, it is shown that one can easily estimate the maximum temperature attained by the particle in the bed. The relation between the maximum interstitial adiabatic temperature and the maximum intraparticle temperature in the reactor is discussed. The computations show that for some sets of parameters in a nonadiabatic reactor, the concentration and temperature profiles are sensitive to small changes in the properties of catalyst particles. The sensitivity of the profiles to the operating conditions, such as overall heat transfer coefficient and initial particle temperature, has been considered by the present author and others (*2, 5, 10* to *12*).

FORMULAS FOR NONISOTHERMAL EFFECTIVENESS FACTORS

The results of Hicks and Weisz (*20*) were presented as plots of η vs. φ for various values of γ, and with β as a variable parameter on each plot. Tinkler and Metzner (*14*) showed that for most practical cases, the value of α would not exceed 2. Carberry (*6*) showed that for $\alpha = \beta\gamma \leq 6$, the η vs. φ curves could be characterized by one parameter, α. It was decided, therefore, to use Carberry's data (*6*) for development of the empirical η, φ relationships which can be used for most practical cases.

First-Order Reaction

For an exothermic first-order irreversible reaction $A \rightarrow B$, Carberry (*6*) showed that for values of the Thiele modulus φ greater than 2.5, η is concisely expressed by

$$\eta = \exp(\alpha/5.0)/\varphi \qquad (1a)$$

where

$$\varphi = \frac{R}{3}\sqrt{\frac{k_v}{D_s}} \qquad (1b)$$

and α is the product of β and γ used by Weisz and Hicks (*20*):

$$\alpha = \beta\gamma = \left[\frac{c(-\Delta H)D_s}{TK_s}\right]\left[\frac{E}{R_g T}\right] \qquad (1c)$$

It is necessary to develop a mathematical expression of η for φ less than 2.5 in order to use the concept of the effectiveness factor in reactor simulation. The success of nonlinear curve fitting techniques depends largely on how

well one can guess at the form of nonlinear functions which will fit the curves. By trial-and-error methods, the following formulas were found to fit the curves in Figure 1 in (6) reasonably well:

$$\text{if } \alpha > 2.5 \text{ and } \varphi < 1.235 - 0.094\alpha \tag{2a}$$

$$\text{or } \alpha \leq 2.5 \text{ and } \varphi < 1.82 - 0.328\alpha \tag{2b}$$

Then

$$\eta = \exp(0.14\varphi\alpha^{1.6}) - 1.0 + \frac{\tanh\varphi}{\varphi} \tag{2c}$$

If the inequality (2a) or (2b) is not satisfied, Equation (1a) derived by Carberry is valid.

It is seen from Equation (2c) that when $\varphi \to 0$, η approaches 1. When $\alpha = 0$ (isothermal case), η equals $\tanh\varphi/\varphi$, which is identical to that derived by Thiele (18). Figure 1a shows the effectiveness factor calculated from Equations (2a) to (2c). The curve *sc* in Figure 1 passes through the intersecting points, $I_0, I_1, \ldots, I_6$, of straight lines and curves corresponding to Equations (1a) and (2c), respectively. The values of α and φ at points I_0-I_6 in Figure 1a are plotted in Figure 1b, and the curve *sc* is approximated by two straight lines s_1 and s_2 from which Equations (2a) and (2b) are derived.

The formula for the effectiveness factor in the case of an endothermic reaction ($\alpha < 0$) is much easier to find than in the exothermic case. From Figure 1 in (6) it can be observed that the effect of endothermic reaction is a displacement of the $\alpha = 0$ (isothermal) curve. Therefore, the following formula can be used:

$$\eta = \frac{\tanh\bar{\varphi}}{\bar{\varphi}} \tag{3a}$$

with

$$\bar{\varphi} = \varphi(1-\alpha)^{0.3} \tag{3b}$$

where φ and α are the same as defined by Equations (1b) and (1c), respectively; and the factor 0.3 was determined by trial and error. The expression for $\bar{\varphi}$ is similar to that used by Weekman and Gorring for the influence of volume change upon the isothermal effectiveness factor (19).

As shown by Weisz and Hicks (20), for values of α greater than 6, there are conditions under which η is not uniquely determined by β, γ, and φ. In these cases, Equation (1a) and (2c) are not valid because the steady state depends on the conditions from which steady state is approached, and the corresponding transient equations should be analyzed (10 to 13). Actually, if such conditions are encountered, one can lower the inlet concentration of the reactant which would decrease the value of α and obtain a stable operation.

Second-Order Irreversible Reaction

By using the same curve fitting techniques as in the case of the first-order reaction, the following formulas are obtained for a second-order reaction, $2A \to B$, from Figure 2 in Carberry's paper (6). For the exothermic case

$$\text{if } \alpha > 3.5 \text{ and } \varphi < 1.15 \tag{4a}$$

$$\text{or } \alpha \leq 3.5 \text{ and } \varphi < -0.043\alpha + 1.3 \tag{4b}$$

Then

$$\eta = \exp(0.133\varphi\alpha) - 1.0 + \frac{\tanh(1.33\varphi)}{1.33\varphi} \tag{4c}$$

If the conditions (4a) or (4b) are not satisfied

$$\eta = \frac{\exp(\alpha/5.0)}{1.33\varphi} \tag{4d}$$

In equations (4a) through (4d)

$$\varphi = \frac{R}{3}\sqrt{\frac{k_v c_s}{D_s}} \tag{4e}$$

and α is the same as defined by Equation (1c). For the endothermic case

$$\eta = \frac{\tanh(1.33\bar{\varphi})}{1.33\bar{\varphi}} \tag{4f}$$

with

$$\bar{\varphi} = \varphi(1-\alpha)^{0.3} \tag{4g}$$

where φ is defined by Equation (4e).

DERIVATION OF EQUATIONS

Steady state equations will be derived for adiabatic and nonadiabatic reactors. It will be considered that these reactors are packed with relatively large spherical catalyst particles (⅛ ft. in diameter, for example) in which significant intraparticle mass concentration and temperature gradients may exist. Fluid is introduced into the bed at $x = 0$, and a first-order irreversible chemical reaction $A \to B$ takes place on the porous surface of the particle. It is assumed that radial and axial dispersions in the fluid can be neglected, so the flow pattern can be approximated by a plug flow.

Case 1: Adiabatic Reactor

If c is the concentration of component A and T is the interstitial fluid temperature, then the steady state mass and heat balances can be described by

$$u\delta\frac{dc}{dx} + (1-\delta)\eta k_v c = 0 \tag{5a}$$

$$u\delta\rho_f c_f\frac{dT}{dx} + (1-\delta)\eta k_v c(\Delta H) = 0 \tag{5b}$$

at

$$x = 0;\ c = c_e,\ T = T_e \tag{5c}$$

where $k_v[=A_0\exp(-E/R_gT)]$ is the intrinsic reaction rate constant per unit of gross volume of catalyst pellet. The effectiveness factor η is given by Equations (1a) to (2c) as functions of φ and α (consequently, as functions of c and T) defined by Equations (1b) and (1c), respectively. Since Equations (5a) to (5c) are nonlinear, a simple mathematical solution would be difficult or impossible to find, so the solution must be obtained by numerical methods.

A heat balance taken over any section including the bed entrance gives

$$c_f\rho_f(T - T_e) = (-\Delta H)(c_e - c) \tag{6a}$$

so that

$$c = c_e - \frac{(T - T_e)c_f\rho_f}{(-\Delta H)} \tag{6b}$$

The temperature and concentration profiles in the reactor can be obtained by numerically solving Equations (5b), (6b), and (1a) to (2c).

The maximum temperature which can exist in an adiabatic reactor can be obtained from Equation (6a) by setting $c = 0$:

$$T_{\max} = T_e + \beta_1 c_e \tag{6c}$$

where

$$\beta_1 = \frac{(-\Delta H)}{c_f\rho_f}$$

As shown by Damköhler (9) and Prater (16), the maximum temperature difference between the external and interior surface of the particle is given by

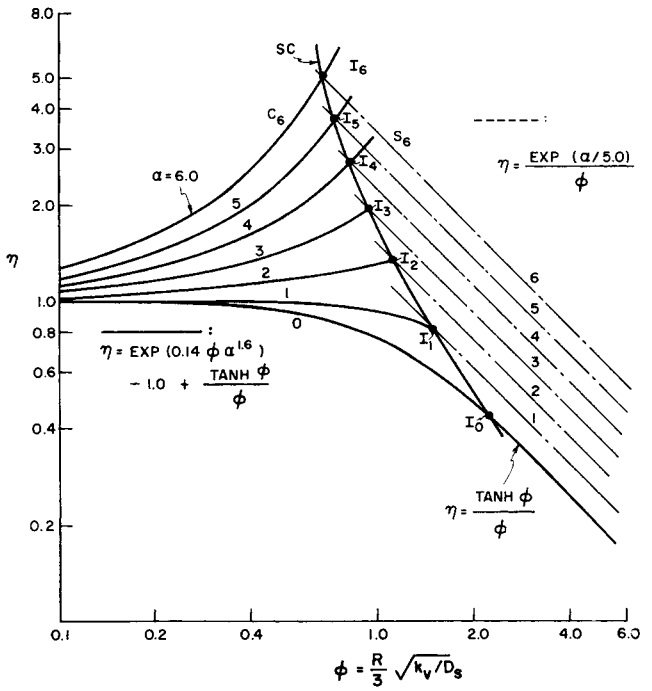

Fig. 1a. Nonisothermal catalytic effectiveness factor.

$$T_{p,\max} = T + \beta_2 c \tag{6d}$$

where

$$\beta_2 = \frac{(-\Delta H) D_s}{K_s}$$

Solving Equation (6a) for T and substituting the result into Equation (6d), one obtains

$$T_{p,\max} = T_e + \beta_1 c_e + (\beta_2 - \beta_1) c \tag{6d'}$$

From Equations (6b) and (6d'), one can construct two straight lines, L_g and L_{p1}, in Figure 2, showing the relation between the fluid concentration c and the fluid temperature T and that between c and the possible maximum particle temperature T_p. $T_{\max}$ obtained from Equation (6c) is also shown in Figure 2.

From Figure 2 it is seen that if

$$\beta_1 \geqq \beta_2$$

or, in terms of physical parameters

$$K_s \geqq D_s c_f \rho_f \tag{6e}$$

then $T_{\max}$, the maximum interstitial adiabatic temperature, is the maximum intraparticle temperature in the reactor. On the other hand, if

$$K_s < D_s c_f \rho_f \tag{6f}$$

then the maximum intraparticle temperature can be greater than the maximum temperature attained by the fluid. The straight line L_{p2} in Figure 2 illustrates this situation, and the intersection $T'_{p,\max}$ of the lines L_{p2} and $c = c_e$ gives the upper bound of the particle temperature. Note that $T'_{p,\max}$ is the maximum intraparticle temperature corresponding to the reactor inlet conditions and can be obtained from Equation (6d) by setting $T = T_e$ and $c = c_e$.

Similarly, for nonisothermal complex reactions

$$\sum_{i=1}^{n} a_{ij} A_i = 0 \quad (j = 1, 2, 3, \ldots, m)$$

one obtains the following equation [see (15) and (17) for derivation] similar to Equation (6d):

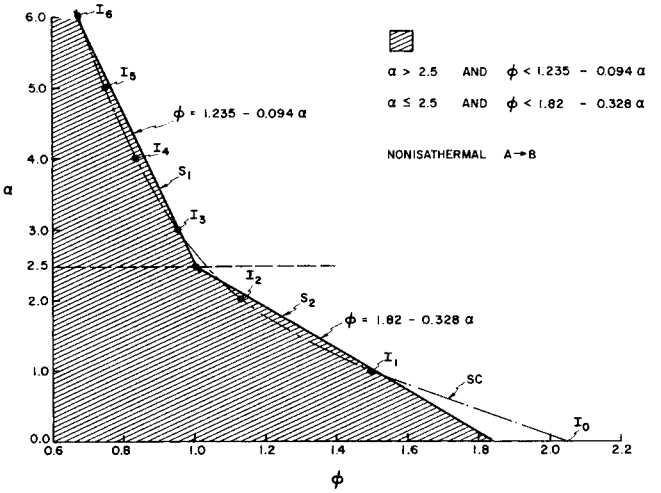

Fig. 1b. α vs. φ.

$$K_s(T_p - T) = \sum_{i=1}^{m} (-\Delta H_i) D_{si} c_i \tag{6g}$$

The heat balance in the fluid can be written

$$c_f \rho_f (T - T_e) = \sum_{i=1}^{m} (-\Delta H_i)(c_{ei} - c) \tag{6h}$$

For the case that all D_{si} are approximately equal to D_s, the following upper bounds for the particle temperature can be obtained. From Equations (6g) and (6h), if

$$\beta_3 \geqq \beta_4 \tag{6i}$$

where

$$\beta_3 = \frac{\sum_{i=1}^{m} (-\Delta H_i) c_{ei}}{c_f \rho_f}, \quad \beta_4 = \frac{D_s \sum_{i=1}^{m} (-\Delta H_i) c_{ei}}{K_s} \tag{6i}$$

then the particle temperature is bounded by the maximum fluid temperature

$$T_{\max} = T_e + \beta_3 \tag{6j}$$

On the other hand, if

$$\beta_3 < \beta_4 \tag{6k}$$

then the particle temperature in the reactor is bounded by the maximum particle temperature corresponding to the reactor inlet conditions

$$T'_{p,\max} = T_e + \beta_4 \tag{6l}$$

Thus, one can estimate the maximum temperature attained by the particle in the reactor without numerical solutions of the differential Equations (5a) and (5b).

Let us define a new Lewis number, the ratio of thermal diffusivity to mass diffusivity, as follows:

$$N_{Le} = \frac{K_s}{D_s c_f \rho_f} \tag{6m}$$

It is interesting to see that the ratios β_1/β_2 and β_3/β_4 are equal to N_{Le}. Therefore, in terms of the Lewis Number, from Equations (6e), (6f), (6i), and (6j) if

$$N_{Le} \geqq 1 \tag{6n}$$

then the maximum interstitial adiabatic temperature is the maximum intraparticle temperature in the reactor. On the other hand, if

$$N_{Le} < 1 \tag{6p}$$

then the maximum intraparticle temperature in the reactor

$$\beta_1 = \frac{(-\Delta H)}{C_t P_f} \qquad \beta_2 = \frac{(-\Delta H) D_S}{K_S}$$

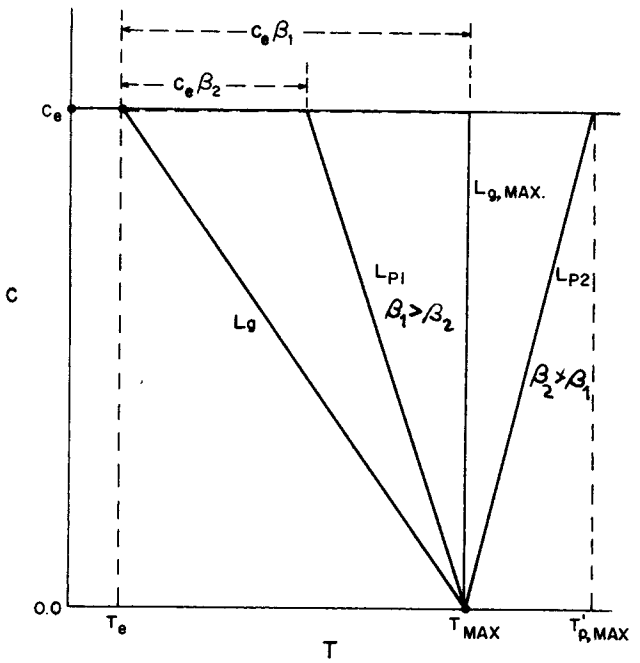

Fig. 2. Graphical illustration of maximum interstitial temperature and maximum intraparticle temperature, adiabatic case.

can be greater than the maximum interstitial adiabatic temperature but is bounded by the maximum intraparticle temperature corresponding to the reactor inlet conditions.

The above criteria are independent of the order of the chemical reactions; therefore, they can be used to estimate the maximum particle temperature attained in an adiabatic reactor without considering the detailed kinetics.

Case 2: Nonadiabatic Reactor

Let R_b be the radius of the reactor, $\overline{U}$ be the reactor overall heat transfer coefficient, and T_w be the ambient temperature; then the conservation equations can be written as (in dimensionless form)

$$\frac{df}{ds} = -a_1\eta A_0 f \exp(-q/y) \tag{7a}$$

$$\frac{dy}{ds} = a_2\eta f A_0 \exp(-q/y) + a_3(y_w - y) \tag{7b}$$

at

$$s = 0; \quad f = 1; \quad y = 1 \tag{7c}$$

where

$$y = \frac{T}{T_e},\ s = \frac{x}{l},\ f = \frac{c}{c_e},\ q = \frac{E}{R_g T_e},\ y_w = \frac{T_w}{T_e}$$

$$a_1 = \frac{(1-\delta)l}{\delta u},\ a_2 = \frac{(1-\delta)lc_e(-\Delta H)}{\delta u c_{fp} \rho_f T_e},\ a_3 = \frac{2\overline{U}l}{uc_{fp}\rho_f R_b}$$

As in the adiabatic case, the effectiveness factor η is a nonlinear function of the interstitial concentration and temperature, described by Equations (1*a*) to (2*c*).

NUMERICAL EXAMPLES AND RESULTS

To examine the effects of intraparticle mass and heat diffusion upon the interstitial concentration and temperature profiles in various types of reactors, equations described in the previous section for a first-order irreversible chemical reaction were solved by using an IBM-7040 digital computer.

Case 1: Adiabatic Reactor

Consider the following numerical example using Equations (5*a*) to (5*c*):

$$\begin{aligned}
\rho_f &= 2.5 \times 10^{-3}\ \text{g./cc.} \\
c_f &= 0.4\ \text{cal./g.} \\
E &= 2.5 \times 10^4\ \text{cal./g. mole} \\
A_0 &= 3 \times 10^7 \\
\delta &= 0.4 \\
(-\Delta H) &= 2.0 \times 10^4\ \text{cal./g. mole} \\
D_s &= 4.0 \times 10^{-3}\ \text{sq.cm./sec.} \\
K_s &= 6.0 \times 10^{-4}\ \text{cal./(cm.)(sec.)(°K.)} \\
C_e &= 2.0 \times 10^{-5}\ \text{g. mole/cc.} \\
T_e &= 600°\text{K.} \\
R &= 0.5\ \text{cm.} \\
l &= 200\ \text{cm.} \\
u &= 20\ \text{cm./sec.}
\end{aligned} \tag{7d}$$

Figure 3 shows the effect of changes in the particle radius upon the steady state interstitial concentration and temperature profiles. The curves E and E' represent the profiles for $R = 0.5$ cm. assuming no intraparticle diffusion effect exists (that is, $\eta = 1$). By comparing the curves E with B and E' with B', respectively, it is seen that the intraparticle diffusion influences the profiles greatly. Figure 4 illustrates how the effectiveness factors for various particle sizes change along the reactor. Near the reactor entrance, η is higher for smaller particles, because, from Equations (1*a*) to (2*c*) or Figure 1, η is indirectly proportional to R for $\varphi > 1$. The smaller the particles, the faster T increases and c decreases, and consequently the faster η decreases. Therefore, as shown in Figure 4, near the reactor outlet the effectiveness factor

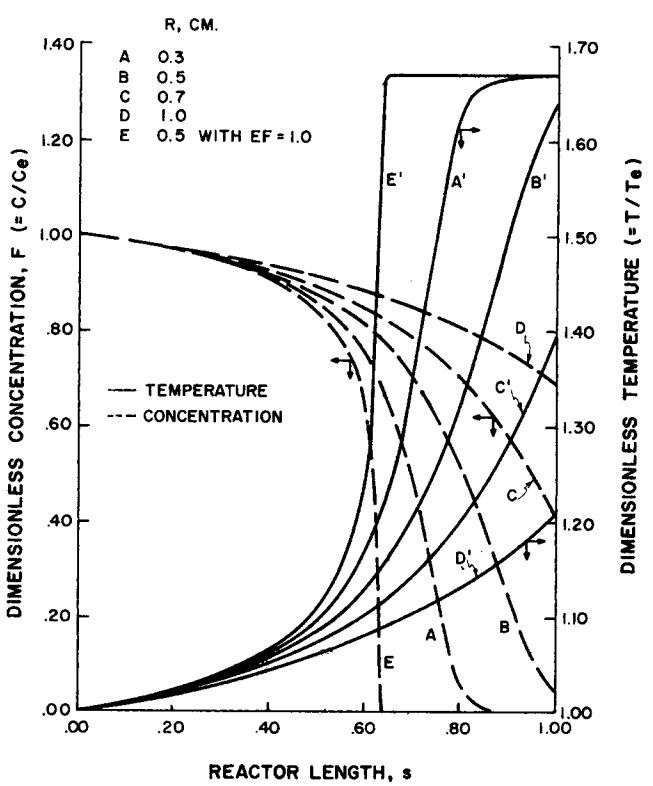

Fig. 3. Temperature and concentration profiles for different particle diameters, adiabatic case.

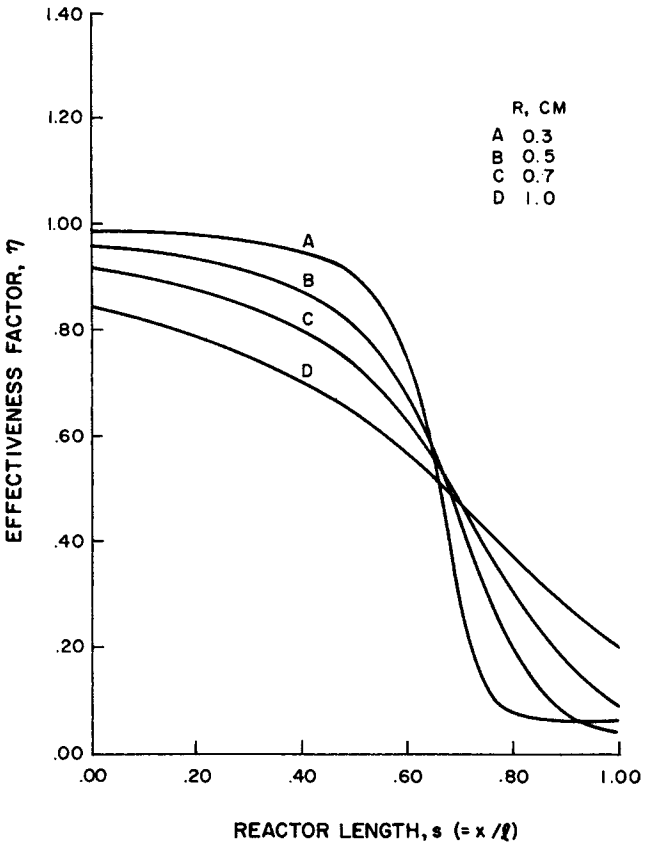

Fig. 4. Effectiveness factor profiles for different particle diameters, adiabatic case.

η is higher for larger particles. In the isothermal case, shown by the curve $\alpha = 0$ in Figure 1*a*, $\alpha = 0$ and $\eta \left(= \dfrac{\tanh \varphi}{\varphi} \right)$ is a monotonically decreasing function of φ, so at every point in the reactor, η is always higher for smaller particles.

Figure 5 illustrates how the concentration and temperature profiles vary with the changes in the effective diffusivity within the catalyst particle. The larger the value of D_s, the smaller the value of φ and the larger the value of α, and consequently the concentration of A decreases to zero in a shorter reactor. Figure 6 illustrates how the profiles vary with the changes in the effective thermal conductivity K_s of the particle. Since α is indirectly proportional to K_s from Equations (1*a*) to (2*c*), η decreases with increasing K_s. The effects of changes in D_s and K upon the reaction rate can be explained from their effects upon the mass and heat transport in the porous particle. If the diffusivity D_s is small, the rate of transport of the component A into the porous particle is relatively low, and, for an irreversible reaction, the reaction rate is lower than in the case without diffusion effect. On the other hand, if the thermal conductivity K_s is small, heat generated by the chemical reaction is trapped within the particle where it raises the temperature and, therefore, increases the rate of reaction.

Case 2: Nonadiabatic Reactor

Let us consider an example for the nonadiabatic case by using the same parameters as in case 1 and in addition by specifying the radius of the reactor, the overall heat transfer coefficient, and the ambient temperature as follows:

$R_b = 5$ cm.
$\overline{U} = 10^{-3}$ cal./(min.)(sq.cm.)
$T_w = 550°$K.

The steady state Equations (7*a*) to (7*c*) and the equations for the effectiveness factor were solved numerically. Figure 7 shows the effect of changes in the particle radius upon the temperature and concentration profiles. If the particle radius is greater than 0.3 cm., the fluid tempera-

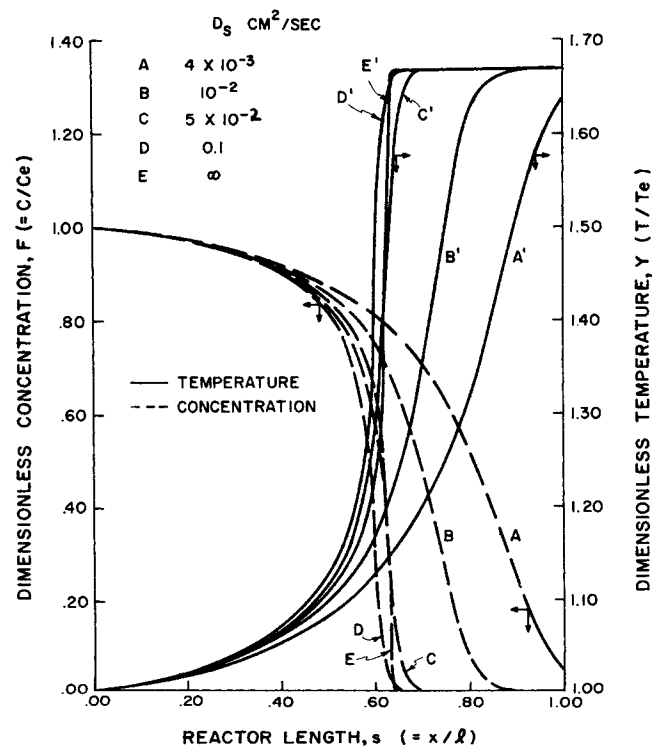

Fig. 5. Temperature and concentration profiles for different effective diffusivities of particles.

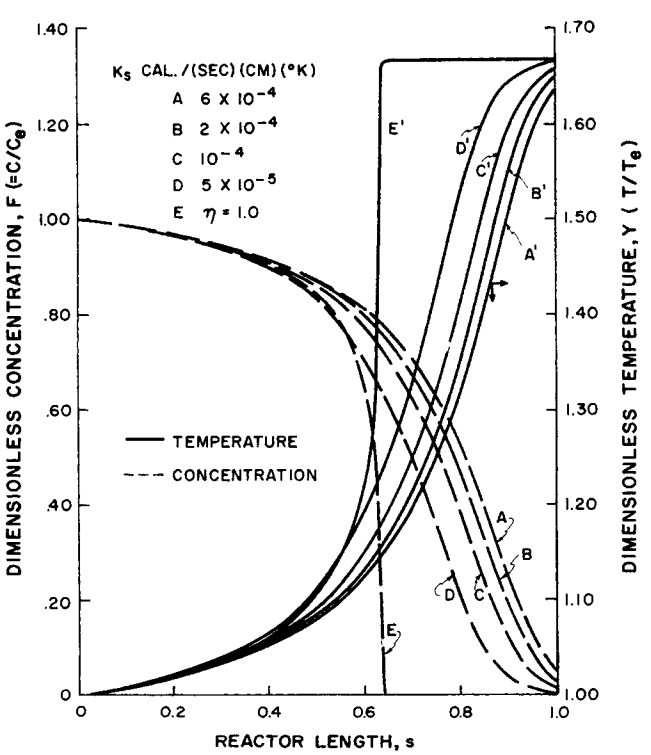

Fig. 6. Temperature and concentration profiles for different thermal conductivities of particles, adiabatic case.

ture decreases along the bed, and the chemical conversion is extremely low. It is seen from Figure 7 that there is a critical change in profiles as the particle radius changes from 0.3 to 0.1 cm. Curves F and F' in Figure 7 are obtained for $R = 0.5$ cm. by assuming the effectiveness factor equal to 1. By comparing curve F with curve c and curve F' with curve c' in Figure 7, it is clear that intraparticle diffusion can have a great effect upon the concentration and temperature profiles. Figure 8 shows the sensitivity of the profiles to the effective diffusivity of the catalyst particles. As shown by curves D and E in Figure 8, a small change in D_s can cause a big change in the effluent concentration and temperature.

From Figures 7 and 8 it is seen that the fluid concentration and temperature profiles and, consequently, the reactor effluent can be very sensitive to small changes in physical properties of particles. Although several authors (*3, 6, 12* to *14*) have discussed the sensitivity of reactor performance to operating conditions such as the overall heat transfer coefficient and initial particle temperature, the sensitivity of reactor performance with respect to the physical properties of particles has not been discussed before. The analysis of reactor sensitivity and an estimate of the maximum temperature for a nonlinear problem in general requires a numerical solution. However, the nature of the solution can be discovered from a qualitative examination of the equations. The following qualitative argument is similar to one used by Aris (*1*).

Equations (7*a*) and (7*b*) can be written as

$$\frac{dw}{ds} = a_1 \eta r(w, y) \tag{8a}$$

$$\frac{dy}{ds} = a_2 \eta r(w, y) + a_3(y_w - y) \tag{8b}$$

where

$$w = 1 - f \tag{8c}$$

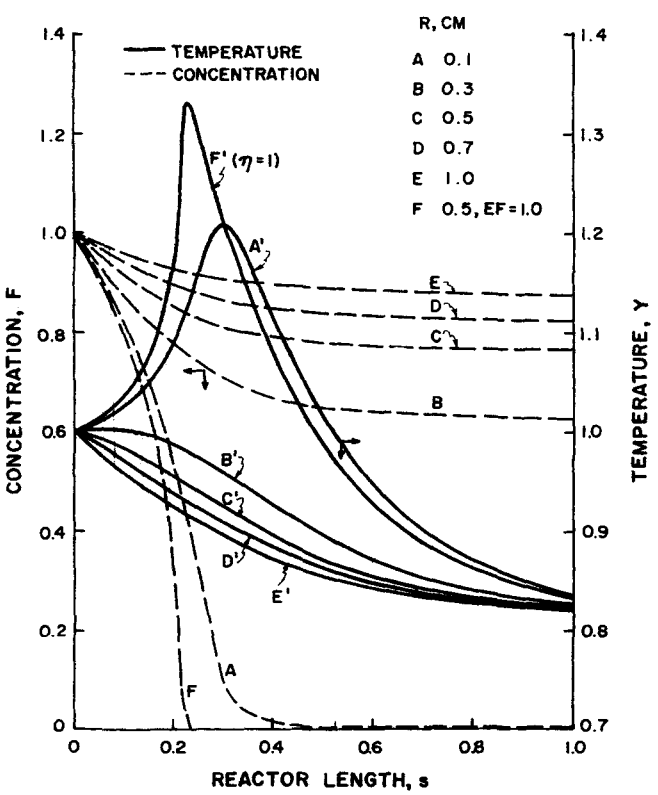

Fig. 7. Effect of particle diameter on temperature and concentration profiles, nonadiabatic case.

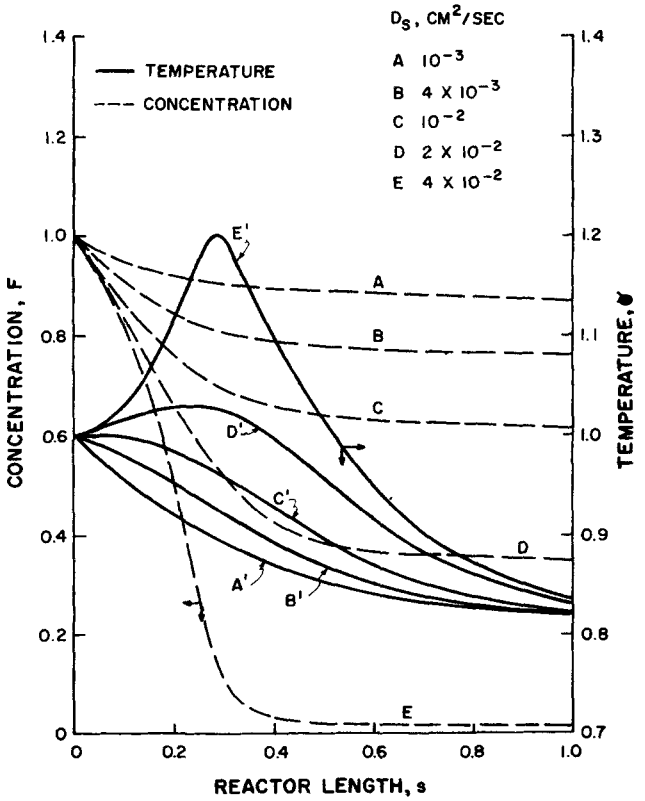

Fig. 8. Effect of effective diffusivity of particle on temperature and concentration profiles, nonadiabatic case.

$$r(w, y) = (1 - w)A_0 \exp(-q/y) \tag{8d}$$

The maximum temperature in the reactor must lie on the locus

$$\frac{dy}{ds} = 0 \tag{9a}$$

Then, from Equation (8*b*)

$$r(w, y) = \frac{a_3}{a_2 \eta}(y - y_w) \tag{9b}$$

By assuming the effectiveness factor η does not vary throughout the reactor and by using Equation (9*b*), the sequence of curves for the loci of maximum temperature is plotted in Figure 9. The curves labeled a to f are for an increasing of η. The straight line L_1 denotes the adiabatic line obtained from Equation (6*a*), and the straight line L_2 represents the corresponding maximum intraparticle temperature calculated from Equation (6c). The dotted curves a' to e' are the reaction paths for an increasing sequence of η. If η corresponds to curves a or b, the inlet temperature y_0 must be the maximum, since dy/ds is always negative. This is the situation for $R = 1.0$ cm. in Figure 7. On the other hand, the reaction path c' intersects with the corresponding loci of maximum temperature at p_1, and a maximum temperature greater than y_0 (though not by so much) is obtained; such is the case for $R = 0.3$ cm. in Figure 7. As η increases, the maximum temperature also increases, and there is a jump in the maximum temperature from p_2 to p_3. Thus, it is reasonable to find a sensitivity such as Figures 7 and 8 show.

Conservative estimates of the maximum temperature, without considering the reaction paths, would be supplied by the intersections of the adiabatic path L_1 with loci for various values of η, as shown by p_1', p_2', and p_3' in Fig-

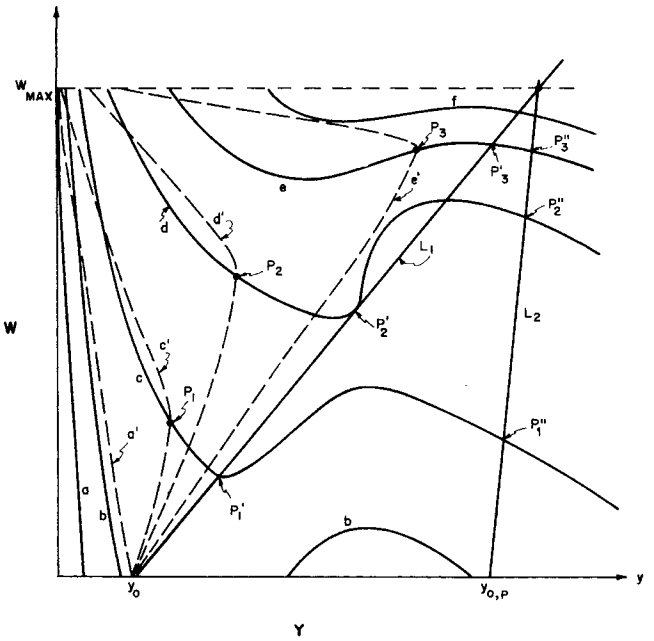

Fig. 9. Loci of maximum temperatures and reaction paths for different η in a nonadiabatic reactor.

ure 9. The intersections of L_2 with the loci, p_1'', p_2'', and p_3'' are the estimates of the maximum intraparticle temperatures for the appropriate η.

CONCLUSIONS

Mathematical formulas were obtained for the catalysts effectiveness factors η for nonisothermal first-order and second-order irreversible chemical reactions. These formulas can be used for most practical cases ($\alpha < 3$). It was shown that if the Lewis number, $N_{Le}\left(=\dfrac{K_s}{D_s C_f \rho_f}\right)$, is greater than or equal to 1, then the maximum interstitial adiabatic temperature is the maximum intraparticle temperature in the reactor. On the other hand, if N_{Le} is smaller than 1, then the maximum intraparticle temperature in the reactor can be greater than the maximum interstitial adiabatic temperature. For some sets of parameters in a nonadiabatic reactor, the concentration and temperature profiles are sensitive to small changes in the properties of catalyst particles.

NOTATION

A, A_i = chemical species
A_0 = frequency factor for k_v
a_{ij} = stoichiometric coefficient
c = concentration of component A
c_i = concentration of the i^{th} species
c_e = influent concentration of component A
c_{ei} = influent concentration of the i^{th} species
c_f = specific heat of gas mixture
D_s = particle effective diffusivity
E = activation energy for chemical reaction
f = c/c_e; dimensionless concentration of component A
$(-\Delta H)$ = heat of reaction
K_s = particle effective thermal conductivity
k_v = $k_s S_v$; intrinsic first-order reaction rate coefficient per unit volume of catalyst pellet
k_s = intrinsic reaction rate constant for surface reaction
l = reactor length
N_{Le} = Lewis number; $K_s/D_s c_f \rho_f$
R = particle radius
R_g = gas law constant
$\hat{R}$ = R_b/R; ratio of the reactor radius to the particle radius
s = x/l; dimensionless reactor length
Λ_s = space interval
s_v = total area of catalyst per unit volume
T = interstitial gas temperature
T_e = influent gas temperature
T_{max} = maximum interstitial gas temperature
$T_{p,max}$ = maximum particle temperature
T_w = ambient temperature
$\overline{U}$ = reactor overall heat transfer coefficient
u = average interstitial velocity
x = axial variable
y = T/T_e; dimensionless gas temperature
y_w = T_w/T_e; dimensionless ambient temperature

Greek Letters

α = $[c(-\Delta H)D_s/TK_s]\,[E/R_gT]$
β = $c(-\Delta H)D_s/TK_s$
β_1 = $(-\Delta H)/c_f\rho_f$
β_2 = $(-\Delta H)D_s/K_s$
β_3 = $\sum_{i=1}^{m}(-\Delta H_i)c_{ei}/\bar{c}_f\bar{\rho}_f$
β_4 = $D_s\sum_{i=1}^{m}(-\Delta H_i)c_{ei}/K_s$
γ = E/R_gT
η = effectiveness factor
$\rho_f, \bar{\rho}_f$ = densities of gas mixtures
δ = bed void fraction
φ = Thiele modulus

LITERATURE CITED

1. Aris, Rutherford, "Introduction to the Analysis of Chemical Reactors," Prentice-Hall, Englewood Cliffs, N. J. (1965).
2. Barkelew, C. H., *Chem. Eng. Progr. Symposium Ser. No. 25*, 55, 37 (1959).
3. Beek, J., *Adv. Chem. Eng.*, 3, 203 (1962).
4. Beskov, V. S., V. P. Kuzin, and M. G. Slinko, *Intern. Chem. Eng.*, 5, 201 (1965).
5. Bilaus, Olegh, and N. R. Amundson, *AIChE J.*, 2, 117 (1956).
6. Carberry, J. J., *ibid.*, 7, 350 (1961).
7. ———, *Chem. Eng. Sci.*, 17, 675 (1962).
8. Cunningham, R. A., J. J. Carberry, and J. M. Smith, *AIChE J.*, 11, 637 (1965).
9. Damköhler, G., *Z. Phys. Chem.*, A193, 16 (1943).
10. Liu, S. L., and N. R. Amundson, *Ind. Eng. Chem. Fundamentals*, 1, 200 (1962).
11. ———, and Aris Rutherford, *ibid.*, 2, 12 (1963).
12. Liu, S. L., and N. R. Amundson, *ibid.*, 2, 183.
13. McGuire, M. L., and Leon Lapidus, *AIChE J.*, 11, 85 (1965).
14. Metzner, A. B., and J. D. Tinkler, *Ind. Eng. Chem.*, 53, 663 (1961).
15. Petersen, E. E., "Chemical Reaction Analysis," Prentice-Hall, Englewood Cliffs, N. J. (1965).
16. Prater, C. D., *Chem. Eng. Sci.*, 8, 284 (1958).
17. Schilson, R. E., and N. R. Amundson, *ibid.*, 13, 237 (1961).
18. Thiele, E. W., *Ind. Eng. Chem.*, 31, 916 (1939).
19. Weekman, V. W., Jr., and R. L. Gorring, *J. Catalysis*, 4, 260 (1965).
20. Weisz, P. B., and J. S. Hicks, *Chem. Eng. Sci.*, 17, 265 (1962).
21. Wendel, M., and C. C. Carberry, *AIChE J.*, 9, 129 (1963).

Manuscript received December 30, 1968; revision received March 7, 1969; paper accepted March 10, 1969. Paper presented at AIChE Los Angeles meeting.